Microbiology (2009), **155**, 3333–3347 **DOI** 10.1099/mic.0.028928-0

Anchoring and length regulation of *Porphyromonas gingivalis* Mfa1 fimbriae by the downstream gene product Mfa2

Yoshiaki Hasegawa,[1] Jun Iwami,[1,2] Keiko Sato,[1]† Yoonsuk Park,[3] Kiyoshi Nishikawa,[1] Tatsuo Atsumi,[1,4] Keiichi Moriguchi,[5] Yukitaka Murakami,[1] Richard J. Lamont,[3] Hiroshi Nakamura,[2] Norikazu Ohno[5] and Fuminobu Yoshimura[1]

Correspondence
Yoshiaki Hasegawa
hyoshi@dpc.agu.ac.jp

[1]Department of Microbiology, School of Dentistry, Aichi-Gakuin University, Nagoya, Aichi 464-8650, Japan

[2]Department of Endodontology, School of Dentistry, Aichi-Gakuin University, Nagoya, Aichi 464-8650, Japan

[3]Department of Oral Biology, University of Florida, Gainesville, FL 32610, USA

[4]Department of Medical Technology, Gifu University of Medical Science, Seki, Gifu 501-3892, Japan

[5]Department of Anatomy, School of Dentistry, Aichi-Gakuin University, Nagoya, Aichi 464-8650, Japan

Porphyromonas gingivalis, a causative agent of periodontitis, has at least two types of thin, single-stranded fimbriae, termed FimA and Mfa1 (according to the names of major subunits), which can be discriminated by filament length and by the size of their major fimbrilin subunits. FimA fimbriae are long filaments that are easily detached from cells, whereas Mfa1 fimbriae are short filaments that are tightly bound to cells. However, a *P. gingivalis* ATCC 33277-derived mutant deficient in *mfa2*, a gene downstream of *mfa1*, produced long filaments (10 times longer than those of the parent), easily detached from the cell surface, similar to FimA fimbriae. Longer Mfa1 fimbriae contributed to stronger autoaggregation of bacterial cells. Complementation of the mutant with the wild-type *mfa2* allele *in trans* restored the parental phenotype. Mfa2 is present in the outer membrane of *P. gingivalis*, but does not co-purify with the Mfa1 fimbriae. However, co-immunoprecipitation demonstrated that Mfa2 and Mfa1 are associated with each other in whole *P. gingivalis* cells. Furthermore, immunogold microscopy, including double labelling, confirmed that Mfa2 was located on the cell surface and likely associated with Mfa1 fimbriae. Mfa2 may therefore play a role as an anchor for the Mfa1 fimbriae and also as a regulator of Mfa1 filament length. Two additional downstream genes (pgn0289 and pgn0290) are co-transcribed with *mfa1* (pgn0287) and *mfa2* (pgn0288), and proteins derived from pgn0289, pgn0290 and pgn0291 appear to be accessory fimbrial components.

Received 6 March 2009
Revised 22 June 2009
Accepted 3 July 2009

INTRODUCTION

Porphyromonas gingivalis is a Gram-negative, black-pigmented, obligate anaerobe that has been implicated in adult periodontitis (Lamont & Jenkinson, 1998; Socransky & Haffajee, 2005), which is a major cause of tooth loss in the adult population. Periodontitis and infection with this organism are also thought to be associated with several systemic diseases, including diabetes, preterm birth, coronary heart disease and atherosclerosis (Dasanayake *et al.*, 2003; Gibson *et al.*, 2006). Fimbriae are one of the major colonization factors of *P. gingivalis*, and contribute to the formation of mixed-species biofilms on oral surfaces (Jenkinson & Lamont, 2005; Kolenbrander *et al.*, 2002; Yoshimura *et al.*, 2009). Fimbriae also play a major role in adhesion to and invasion of gingival epithelial cells by *P. gingivalis* (Andrian *et al.*, 2006; Lamont & Jenkinson, 1998).

†Present address: Department of Developmental and Reconstructive Medicine, Nagasaki University Graduate School of Biomedical Sciences, Nagasaki 852-8588, Japan.

Abbreviations: CBB, Coomassie brilliant blue R-250; GST, glutathione *S*-transferase.

The GenBank/EMBL/DDBJ accession number for the *mfa2* sequence of *P. gingivalis* ATCC 33277 is AB360435.

P. gingivalis has at least two types of fimbriae, namely FimA and Mfa1 fimbriae, following the names of their major subunit proteins, whose gene loci are separated from each other on the chromosome (Hamada *et al.*, 2002; Ogawa *et al.*, 1994; Yoshimura *et al.*, 1984, 1989). Well-characterized strains such as ATCC 33277 and 381 have been shown to express both fimbriae types (Hayashi *et al.*, 2000; Naito *et al.*, 2008; Park *et al.*, 2005; Yoshimura *et al.*, 1989). However, neither fimbriae type is produced in the sequenced strain W83 (Nelson *et al.*, 2003; Suzuki *et al.*, 1988; Yoshimura *et al.*, 1989). There are several reports describing a third type of fimbria or an outer membrane protein of 53 kDa in 381 (Arai *et al.*, 2000; Hongyo *et al.*, 1997, 1998). This protein seems to have a strong homology with Mfa1 fimbriae, although the extent to which this is distributed among *P. gingivalis* strains remains to be established (Murakami *et al.*, 2002; Yoshimura *et al.*, 1989). The Mfa1 fimbriae have been less characterized than the FimA fimbriae, partly because the former appear to be much shorter filaments than the latter, and are difficult to purify (Hamada *et al.*, 1996; Ogawa *et al.*, 1995). In later studies, Mfa1 fimbriae were purified from lysed cells of a *fimA* mutant and found indeed to be short filaments of uniform length (average 103 nm) (Park *et al.*, 2005). Very little is known about the function(s) of Mfa1 fimbriae, although recent reports show that Mfa1 fimbriae are involved in coadhesion with *Streptococcus gordonii* (Chung *et al.*, 2000; Lamont *et al.*, 2002; Park *et al.*, 2005), autoaggregation and colonization (Lin *et al.*, 2006), and, like FimA fimbriae, they can stimulate potent inflammatory responses (Hajishengallis *et al.*, 2002; Hiramine *et al.*, 2003; Takahashi *et al.*, 2006).

During the course of isolation and purification of Mfa1 and FimA fimbriae from various strains, we found that an *mfa1* mutant complemented by the introduction of the wild-type *mfa1* gene *in trans* (cSMF1) (Park *et al.*, 2005) had an aberrant phenotype and produced Mfa1 fimbriae as long filaments, loosely attached to and therefore easily shed from the cells, similar to the FimA fimbriae of strains ATCC 33277 or 381. Based on these observations and our previous finding that *mfa1* and the adjacent downstream gene pg0179 (equivalent to pgn0288 in 33277) (Naito *et al.*, 2008) are co-transcribed (Chung *et al.*, 2000), we hypothesized that cSMF1 has a defect in the downstream gene, and that this defect causes the aberrant Mfa1 fimbrial phenotype, presumably due to a polar effect of the insertional mutation in cSMF1 (Lamont *et al.*, 2002), which is complemented with *mfa1* only (Park *et al.*, 2005). Here, we report the characterization of the pgn0288 gene (hereafter designated *mfa2*) downstream of *mfa1* and its protein product in ATCC 33277.

METHODS

Bacterial strains and growth conditions. All *P. gingivalis* and *Escherichia coli* strains used in this study are listed in Table 1. *P. gingivalis* ATCC 33277 (33277) and its derivatives were grown on blood agar plates [Brucella HK agar base (Kyokuto) supplemented with 5 % (w/v) laked rabbit blood, 2.5 μg haemin ml^{-1}, 5.0 μg menadione ml^{-1} and 0.01 % (w/v) DTT] at 37 °C under anaerobic conditions [10 % (v/v) CO_2, 10 % (v/v) H_2 and 80 % (v/v) N_2]. Cells were cultivated in sTSB liquid medium [trypticase soy broth supplemented with 0.25 % (w/v) yeast extract, 2.5 μg haemin ml^{-1}, 5.0 μg menadione ml^{-1} and 0.01 % (w/v) DTT] or general anaerobic GAM broth (Nissui) at 37 °C for 30–48 h under anaerobic conditions. When necessary, chloramphenicol (Cm; 4 μg ml^{-1}), erythromycin (Em; 10 μg ml^{-1}) or tetracycline (Tc; 2 μg ml^{-1}) was added to the medium. *E. coli* strains were grown in Luria–Bertani medium supplemented, when necessary, with ampicillin (100 μg ml^{-1}), kanamycin (50 μg ml^{-1}) or erythromycin (200 μg ml^{-1}).

DNA manipulations. Standard techniques were used for purification and manipulation of DNA (Nagano *et al.*, 2005; Nishiyama *et al.*, 2007). Restriction endonucleases, DNA ligase and related enzymes were purchased from Takara Bio or New England Biolabs. The Zero Blunt TOPO PCR cloning kit was from Invitrogen. The oligonucleotides used for PCR or RT-PCR were synthesized by Sigma Genosys. DNA sequencing was carried out using the ABI PRISM version 1.1 kit and ABI PRISM 3100-Avant Genetic Analyzer (Applied Biosystems). Constructs for generating mutants or recombinant protein production were sequenced to rule out unintended base changes.

Construction of *P. gingivalis* mutant and complementation strains. The *mfa2* gene (pgn0288) downstream of *mfa1* was amplified as an approximately 1.6 kb fragment from the 33277 chromosome by PCR using primers AGU-101F and AGU-101R (see Table 2 for primer sequences), designed based on the sequence of corresponding gene pg0179 in the *P. gingivalis* W83 genome (Nelson *et al.*, 2003). The amplified fragment was cloned into the plasmid vector pCR-TOPO with the Zero Blunt TOPO PCR cloning kit to construct pCRJI-2 (Table 1). This was used for sequencing *mfa2* and for construction of the *mfa2* mutant.

A *fimA* mutant (JI-1) was constructed by the PCR-based overlap extension method as described previously (Nagano *et al.*, 2005). An *mfa2* mutant (JI-2) that had an *ermF–ermAM* cassette (Fletcher *et al.*, 1997) insertion at the *Nae*I site (50 bp) in the *mfa2* coding region cloned in pCRJI-2 was constructed as described previously (Hasegawa *et al.*, 2003; Hongo *et al.*, 1999). A *fimA* and *mfa2* double mutant (JI-12) was also constructed by the same techniques. The complemented strains JI-3 and JI-4 were constructed by the introduction of an expression vector, pTCBex-*mfa2*, a pT-COW derivative (Gardner *et al.*, 1996). In brief, the entire coding region of *mfa2* in 33277 was amplified by PCR using AGU-102BF and AGU-102HR with *Bam*HI and *Hin*dIII tags, respectively, and the resulting fragment was then cloned downstream of the *fimR* promoter region in pTCBex (Nagano *et al.*, 2007), digested with the appropriate enzymes. The resulting vector pTCBex-*mfa2* was transferred into *P. gingivalis* JI-2 or JI-12 via conjugation from *E. coli* S17-1. *P. gingivalis* with pTCBex (empty vector) was used as a negative control where appropriate, although these data are not shown.

Production of recombinant protein. To construct a plasmid expressing recombinant Mfa2, the region of *mfa2* encoding the putative mature product (nucleotides 121–975) without the N-terminal leader sequences was amplified by PCR using AGU-103BF and AGU-103SR. The resulting fragment was cloned into expression vector pGEX-6P (GE Healthcare Bio-science), yielding plasmid pGEX-′Mfa2 encoding glutathione *S*-transferase (GST)-fused recombinant Mfa2 (GST-r′Mfa2). The plasmid was introduced into *E. coli* strain BL21 for overproduction and purification of GST-r′Mfa2.

Preparation of cellular fractions. *P. gingivalis* strains were anaerobically cultured for 24–48 h, and cells were harvested by

Table 1. Strains and plasmids used in this study

Strain or plasmid	Relevant characteristics*	Source or reference
***P. gingivalis* strains**		
ATCC 33277	Type strain, producing both FimA and Mfa1 fimbriae, Gm^r	ATCC
SMF1	Derivative of ATCC 33277 with an insertional inactivation of the *mfa1* gene, Em^r	Lamont *et al.* (2002); Park *et al.* (2005)
JI-1	Derivative of ATCC 33277 with *fimA* deletion by *cat*, Cm^r	This study
JI-2	Derivative of ATCC 33277 with an insertional inactivation of the *mfa2* gene, Em^r	This study
JI-3	JI-2 containing pTCBex-*mfa2*, a complemented strain, Em^r, Tc^r	This study
JI-12	Derivative of JI-2 with *fimA* deletion by *cat*, Em^r, Cm^r	This study
JI-4	JI-12 containing pTCBex-*mfa2*, a complemented strain, Em^r, Cm^r, Tc^r	This study
***E. coli* strains**		
DH5 α	F^- ϕ80*lacZ* ΔM15 Δ(*lacZYA-argF*) U169 *deoR recA1 endA1 hsdR17*(r_k^-,m_k^+) *phoA supE44* l^- *thi-1gyrA96 relA1*	Takara
BL21	F^- *ompT hsd*S_B (r_B^-,m_B^-) *gal dcm araB*::T7 RNAP-*tetA*	GE Healthcare Bio-Science
S17-1	$RecA^-$, ΩRP4-Tc::Mu-Kn::T7), Tp^r	Gardner *et al.* (1996)
TOP10	F^- *mcrA* Δ(*mrr-hsdRMS-mcrBC*) F80*lacZ* ΔM15 Δ*lacC74 recA1 araD139* Δ(*ara-leu*) *7697 galU galK rpsL* (Str^r) *endA1 nupG*	Invitrogen
Plasmids		
pCR-TOPO	Cloning vector, Km^r	Invitrogen
pCRJI-2	pCR-TOPO derivative carrying a 1.6 kb fragment containing *mfa2*	This study
pVA2198	Plasmid used for a drug cassette, *ermF-ermAM*, Em^r	Fletcher *et al.* (1997)
pTCBex	Derivative of pT-COW, an expression vector, containing the promoter region of *fimR*, Ap^r in *E. coli*, Tc^r in *P. gingivalis*	Nagano *et al.* (2007)
pTCBex-*mfa2*	pTCBex derivative carrying the coding region of *mfa2*, Ap^r in *E. coli*, Tc^r in *P. gingivalis*	This study
pGEX-6P	GST gene fusion and expression vector, Ap^r	GE Healthcare Bio-Science

*ATCC, American Type Culture Collection; Gm^r, gentamicin resistance; *cat*, chloramphenicol acetyltransferase; Cm^r, chloramphenicol resistance; Em^r, erythromycin resistance; Tc^r, tetracycline resistance; Tp^r, trimethoprim resistance; Km^r, kanamycin resistance; Ap^r, ampicillin resistance.

centrifugation, washed once, and disrupted by chemical reagents (BugBuster, Novagen) for immunoprecipitation, sonication (Nagano *et al.*, 2005) or in a French pressure cell (Park *et al.*, 2005). Undisrupted cells were removed by centrifugation at 1000 ***g*** for 10 min. The supernatant was used as a whole-cell lysate. The envelope was collected as a pellet by centrifugation of whole-cell lysate at

Table 2. Primers for PCR and RT-PCR used in this study

Primer	Sequence (5′ to 3′)*	Relevant information
AGU-101F	GGGAAGATCATAATACAAATGAGG	For mutation of *mfa2*
AGU-101R	ACTCGCTTTCCCCTCTTTCT	
AGU-102BF	TTTTAAAACAGGATCCATGAACAAACGGAAGCATAT	For complementation of *mfa2*
AGU-102HR	CTTTTTTCTCAAGCTTTTAAAGTTCTATTTCGTAAC	
AGU-103BF	GTGGATCCCCTCGAGGAGTATATGTCAA	For production of recombinant Mfa2
AGU-103SR	TCGTCGACTTAAAGTTCTATTTCGTAAC	
mfa1F_RT	GTTCTGTTTTGGCTACCATTACG	For RT-PCR of *mfa1*
mfa1R_RT	TTGATGCTCTTGATGTGGATATG	
mfa2F_RT	AATGTGTTTGAGGATGTCCAGTT	For RT-PCR of *mfa2*
mfa2R_RT	CATTGATACAGCGCAAGTTGATA	
0289F_RT	ATATCGTGGAAGGAGTGGAAAAT	For RT-PCR of pgn0289
0289R_RT	ATAAACCTCCAGATAGGCAGAGC	
0290F_RT	TACGCTATGAAAGGAATCAAGGA	For RT-PCR of pgn0290
0290R_RT	GTAACAATCCGTAGTGCCGTTAC	
0291F_RT	TAACAGTACCTGTCGATGTGGTG	For RT-PCR of pgn0291
0291R_RT	TCTCGTCTGTAGCGGTTAGTTTC	

*Underlined sequences in AGU-102BF, AGU-102HR, AGU-103BF and AGU-103SR indicate *Bam*HI, *Hin*dIII, *Bam*HI and *Sal*I sites, respectively.

100 000 ***g*** for 60 min at 4 °C and washed once as described previously (Nagano *et al.*, 2005). The outer and inner membranes were separated by the differential extraction method (Murakami *et al.*, 2002).

Purification and preparation of fimbriae, proteins and antibody. Mfa1 fimbriae were purified from JI-1 (Δ*fimA*) as described previously (Park *et al.*, 2005), except for the absence of detergent. FimA fimbriae and Mfa1 fimbriae were purified from washing solutions of SMF1 and JI-12 (Δ*fimA* and Δ*mfa2*), respectively (Yoshimura *et al.*, 1984). Purification of GST-r′Mfa2 was carried out with a GST affinity column (Glutathione Sepharose 4B, GE Healthcare Bio-science), following the manufacturer's instructions. Purity was examined by SDS-PAGE and Coomassie brilliant blue R-250 (CBB) staining. Protein concentration was measured by using the Micro BCA Protein Assay kit (Pierce Biotechnology). Polyclonal antibody against Mfa1 and GST-r′Mfa2 was raised in rabbits as described previously (Sakakibara *et al.*, 2007; Yoshimura *et al.*, 1989). Another specific antiserum against Mfa1 for double labelling immunogold microscopy was raised in chickens. Briefly, purified Mfa1 protein obtained by dissection of bands in SDS-PAGE gels using pure Mfa1 fimbriae was mixed with Freund's complete adjuvant, and the mixture was injected into chickens subcutaneously four times at 2-week intervals.

SDS-PAGE and Western immunoblotting. SDS-PAGE and Western immunoblotting were carried out as described previously (Murakami *et al.*, 2002; Nagano *et al.*, 2005). Proteins were separated with a 12 % (w/v) SDS-PAGE gel and visualized by staining with CBB. For Western immunoblotting, proteins were transferred onto a nitrocellulose membrane (Hybond ECL nitrocellulose membrane, GE Healthcare Bio-science) and detected by using antibody raised against Mfa1 (Yoshimura *et al.*, 1989) or Mfa2 and peroxidase-conjugated goat anti-rabbit IgG (MP Biomedicals). Signals were visualized with 0.01 % (w/v) 4-chloro-1-naphthol in 20 mM Tris/HCl (pH 7.5) containing 0.5 M NaCl supplemented with hydrogen peroxide (Nagano *et al.*, 2005). To increase sensitivity for detection, ECL Plus Western immunoblotting detection reagents (GE Healthcare Bio-science) were used for visualization according to the manufacturer's instructions.

Detection of Mfa1 fimbrilin, minor components and Mfa2 protein. Mfa1 in whole culture, cells and culture supernatant was detected after precipitation with cold TCA, as described previously (Hongo *et al.*, 1999), except for the use of 2 M Tris to neutralize samples. Minor components of Mfa1 fimbriae and Mfa2 were detected by CBB dye staining and Western immunoblotting after SDS-PAGE.

Protein analysis by MS. The minor components of Mfa1 fimbriae were identified by MALDI-TOF MS (Masuda *et al.*, 2006). CBB-stained protein bands were excised and digested with trypsin. The peptides were extracted and concentrated, and analysed using a 4800 MALDI TOF/TOF analyser (Applied Biosystems). The identities of the proteins were deduced from MS peaks via the peptide mass fingerprinting methods in Mascot (http://www.matrixscience.com/). The proteins were identified according to the significance criteria of the search program ($P<0.05$).

Electron microscopy. *P. gingivalis* cells and fimbriae were examined with a transmission electron microscope (Carl-Zeiss LEO LIBRA120 or JEM-1200EX, JEOL). An aliquot (10 μl) of bacterial culture or the purified fimbriae was placed on a high-resolution carbon substrate (Ohkenshoji). Then samples were negatively stained with 1 % (w/v) ammonium molybdate for 2 min. For immunogold staining, bacterial cells were fixed with 4 % (w/v) paraformaldehyde in 0.1 M PBS, pH 7.4, at 37 °C for 1 h. The specimens were dehydrated, immersed in L-R White (London Resin), and embedded in gelatin capsules. The resin was polymerized at 55 °C for 24 h. Ultra-thin sections were cut and collected on 400-mesh nickel grids (Ohkenshoji). The sections were incubated with 1 % (w/v) BSA in PBS (BSA/PBS) for 30 min at room temperature, then incubated with anti-rMfa2 rabbit antiserum overnight at 4 °C, followed by washing with PBS. The sections were then incubated in anti-rabbit IgG labelled with 20 nm gold (EY Laboratories), diluted in BSA/PBS (1 : 50), followed by incubation for 1 h and washing with PBS. Chicken antiserum against Mfa1 and goat anti-chicken Ig conjugated with 6 nm gold particles (Abcam) were used for double-labelling experiments. Then they were fixed again with 2 % glutaraldehyde, and stained with uranyl acetate and lead citrate. The samples were observed under a JEM-1210 electron microscope (JEOL).

Autoaggregation assay. Cells were grown as described above, harvested by centrifugation at 8000 ***g*** for 10 min, gently washed once with PBS (pH 6.0), and suspended in the same buffer. The OD_{600} value of the cell suspension was measured and adjusted by dilution with the buffer to 1.0. Aliquots (2 ml) in test tubes (13 mm diameter) were shaken at 37 °C at a speed of 130 strokes per minute. At various time points, OD_{600} values of the suspension were measured with a spectrophotometer (CO8000 cell density meter).

Total RNA isolation and RT-PCR. Total RNA was isolated from *P. gingivalis* 33277 by the RiboPure-Bacteria kit (Ambion). The extracted RNA was treated with RNase-free DNase I (Ambion). Superscript III (Invitrogen) was used to generate cDNA from RNA (1 μg) templates with a random primer, as described by the manufacturer. The resulting cDNA was used as a template for following standard PCR (Takara Ex Taq). The primers used for standard PCR (Table 2) were specific for the *mfa1*, *mfa2*, pgn0289, pgn0290 or pgn0291 genes. Controls without reverse transcriptase were included in all experiments.

Immunoprecipitation assay. Immunoprecipitation assays were performed to determine the interaction between Mfa1 and Mfa2 by using the ProFound co-immunoprecipitation kit based on a direct immobilization of an antibody to aldehyde-activated, beaded agarose (Pierce Biotechnology). Briefly, a 33277 cell pellet was lysed with BugBuster (Novagen) containing proteinase inhibitors. Anti-Mfa2, anti-Mfa1 or anti-OmpA (Pgm6/7) antiserum (Nagano *et al.*, 2005) was immobilized on the agarose gel beads, washed, and incubated overnight with whole-cell lysate at 4 °C. Beads were then washed and resuspended in SDS-PAGE loading buffer. Samples were separated by SDS-PAGE, and Western immunoblotting was performed with anti-Mfa2 or anti-Mfa1 antiserum.

RESULTS

Genes downstream of *mfa1* in ATCC 33277

In this study we focused on the *mfa1* gene, encoding the major subunit (fimbrilin) of Mfa1 fimbriae, and genes downstream of *mfa1*. The complete genome sequences of 33277 and strain W83 are now available (Naito *et al.*, 2008; Nelson *et al.*, 2003). Since *mfa1* in W83 is interrupted by an insertion sequence, to study Mfa1 fimbriae, we have used 33277 expressing both FimA fimbriae (Yoshimura *et al.*, 1984) and Mfa1 fimbriae (Park *et al.*, 2005), which present morphologically as long and short filaments, respectively. Sequencing of *mfa2* (corresponding to pgn0288 in 33277 or pg0179 in W83) was carried out in 33277 [our sequence data for *mfa2* (pgn0288) was matched completely to *mfa2*

in the 33277 genome database], and the sequence of a further downstream region from *mfa2* was taken from the 33277 genome database. At least five genes (*mfa1* to pgn0292) prior to *ragA* with the same transcriptional direction were found at this locus in 33277, and thus represent a possible gene cluster for Mfa1 fimbriae (Fig. 1). In contrast, W83 appears to have nine ORFs prior to *ragA*, including IsPg4 (pg0177) disrupting *mfa1*, pg0183 and IsPg1 (pg0184). Among these, pg0183 is not present in 33277 (Hall *et al.*, 2005). *mfa2* has a high homology (98 % at the DNA level) between 33277 and W83. BLASTP analysis showed that Mfa2 has some homologies to corresponding regions of ORFs immediately downstream of *fimA* [comprising pgn0181 (29 % identity and 49 % similarity at the N-terminal region in 33277) and pg2133 (26 % identity and 43 % similarity at the N-terminal region in W83)]. Mfa2 showed homology to the hypothetical protein BT1062 of *Bacteroides thetaiotaomicron* VPI-5482 (E value 8×10^{-12}) and the hypothetical protein BF2211 in *Bacteroides fragilis* YCH46 (E value 6×10^{-11}) in the global value, but the function of Mfa2 could not be predicted.

Characterization of a mutant deficient in *mfa2* and its complementation strain

A knockout mutant of *mfa2* and its complemented strain were constructed. The mutant JI-2 had *mfa2* disrupted with an antibiotic resistance cassette, and the complemented strain JI-3 carried an expression vector pTCBex-*mfa2* in JI-2 (Nagano *et al.*, 2007). Furthermore, to perform the morphological study of Mfa1 fimbriae, we constructed another *mfa2* mutant, JI-12 (Δ*fimA* and Δ*mfa2*), and its *mfa2*-complemented strain JI-4 (see Methods). The presence and location of Mfa1 fimbriae in the *mfa2* mutant JI-2 strain were investigated. In the absence of Mfa2, retention of Mfa1 fimbriae on the cells was diminished, and Mfa1 fimbriae appeared mostly in the cell supernatant (Fig. 2a, b, lane 2 in Sup). The complemented strain JI-3 demonstrated a phenotype similar to the parent, with Mfa1 fimbriae firmly bound to the cell surface and absent from the supernatant (Fig. 2a, b, lane 3 in Sup). Total expression levels of Mfa1 fimbriae among the parental, JI-2 and JI-3 strains were consistent (Fig. 2b, lanes 1–3 in Cells + Sup), as determined by

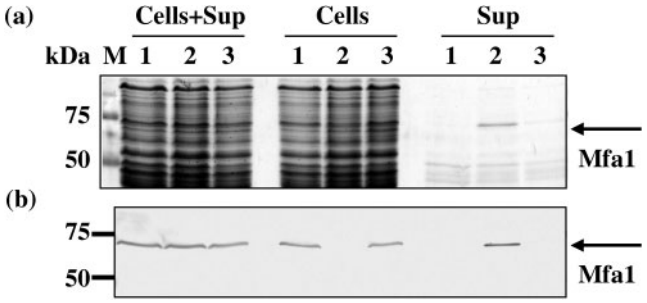

Fig. 2. Unusual distribution of filaments of the Mfa1 fimbriae in the *mfa2* mutant. (a) Partial protein profile of the parental 33277 (lane 1), *mfa2* mutant JI-2 (lane 2) and complemented mutant strain JI-3 (lane 3). Whole cultures (Cells + Sup), cells and culture supernatants (Sup) were treated with cold TCA in order to recover all proteins and to destroy intrinsic, strong proteolytic activities of this organism (Nishiyama *et al.*, 2007). The TCA precipitates were neutralized and separated by SDS-PAGE, followed by CBB staining. (b) Western immunoblotting of panel (a) using anti-Mfa1 serum. A band in lane 2 in Sup of (a), indicated by an arrow, was identified as Mfa1 by antiserum [lane 2 in Sup of (b)].

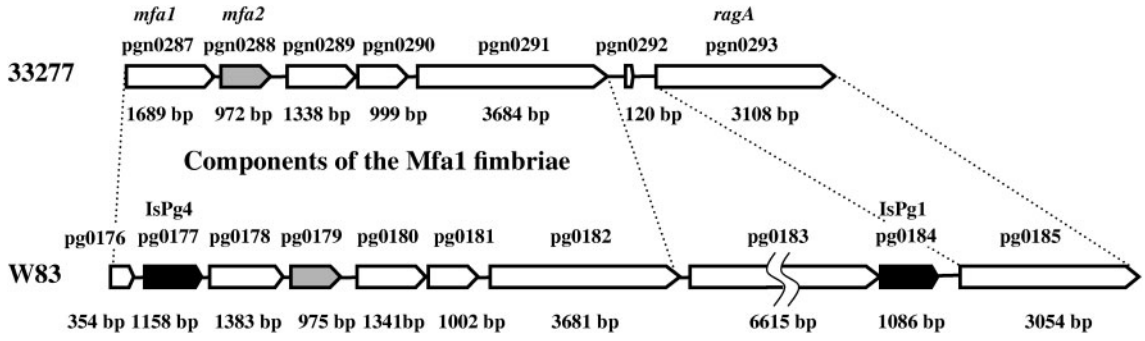

Fig. 1. Mfa1 fimbriae-associated genes in *P. gingivalis* ATCC 33277. Mfa1 fimbrial genes in 33277 are shown in parallel with those in W83. The *mfa1* gene has been previously sequenced in ATCC 33277 and 381 and deposited as a 67 kDa fimbrilin and a cell surface protein (AB016284 and D28770), respectively (Hamada *et al.*, 2002; Ogawa *et al.*, 1994), although the corresponding gene of W83 is split into pg0176 and pg0178 by insertion of pg0177 (ISPg4, transposase) (Park *et al.*, 2005). W83 produces neither FimA nor Mfa1 fimbriae, presumably due to disruption of *fimS* (Hayashi *et al.*, 2000) and *mfa1*, respectively. The *mfa2* gene (annotated as pgn0288 in 33277 or pg0179 in W83, indicated by the grey bars with pointed ends) in 33277 was sequenced in this study, and the 33277 genome database was utilized for the sequence of genes downstream of *mfa2*. The gene products of pgn0289, pgn0290 and pg0291 were identified as minor components of pure Mfa1 fimbriae in JI-1 (Δ*fimA*) by MALDI-TOF MS, as described in the text (and also shown in Fig. 3, Table 3).

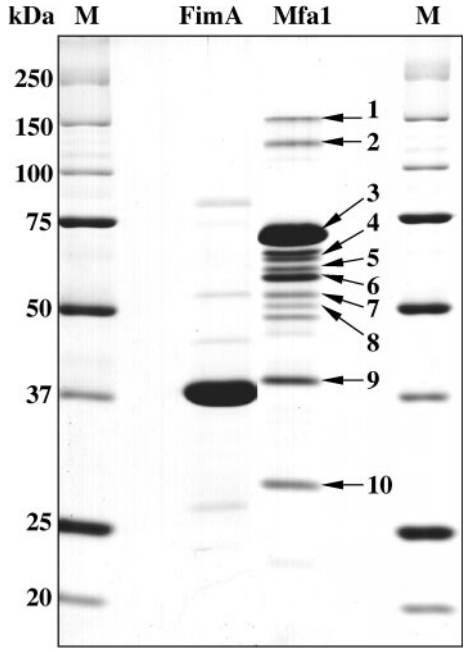

Fig. 3. Identification of the minor components of the Mfa1 fimbriae. A typical SDS-PAGE pattern of highly purified *P. gingivalis* Mfa1 fimbriae is shown together with that of FimA fimbriae. Both FimA (lane FimA) and Mfa1 fimbriae (lane Mfa1) were purified without using any detergent from the mutants SMF1 (Δ*mfa1*) and JI-1 (Δ*fimA*), respectively. Protein bands are numbered from 1 to 10 together with arrows to identify them by MALDI-TOF MS (see also Table 3).

densitometric analysis of the Mfa1 protein bands present in the cell and supernatant fractions (data not shown). Furthermore, numerous long filamentous structures and some vesicles were observed in the culture supernatant from JI-12 (Δ*fimA* and Δ*mfa2*) by electron microscopy (data not shown).

Analysis of minor/accessory proteins in Mfa1 fimbriae and localization of Mfa2

The Mfa1 fimbriae could be purified from whole-cell lysate of 33277 or its *fimA*-defective mutant JI-1 by complete cell disruption using a French pressure cell, as described in Methods. They were not washed from the cell surface by the mild washing method that removes FimA fimbriae (Yoshimura *et al.*, 1984).

A major band (74 kDa) and at least nine minor protein bands were detected in Mfa1 fimbriae purified from JI-1 (Δ*fimA*), when a large amount of the fimbriae was applied (Fig. 3, lane Mfa1). The major and minor protein bands were cut from gels and analysed using MALDI-TOF MS. All the proteins were identified through searching the NCBI database for peptide mass fingerprinting as follows. Bands 1 and 2 (approximately 150 and 130 kDa, respectively) were gene products of pgn0291 in 33277 that have a conserved amino acid sequence of von Willebrand factor A in an N-terminal region, bands 3–8 including the major band (74–50 kDa) were all matched to a gene product of pgn0287 (annotated as the 67 kDa major outer membrane protein that is an earlier name for Mfa1) (Ogawa *et al.*, 1994), band 9 (40 kDa) was a putative lipoprotein (corresponding to pgn0289), and band 10 (30 kDa) was antigen PG49 (corresponding to pgn0290), interestingly indicating that all the minor bands were gene products either of *mfa1* or its downstream genes pgn0289, pgn0290 and pgn0291, as shown in Table 3. Therefore, Mfa1 fimbriae appear to have at least three minor components, associated with the major protein, expressed

Table 3. Identification of proteins by MALDI-TOF MS peptide mass fingerprinting

Protein number*	Probability†	Description (corresponding CDS‡ number in *P. gingivalis* ATCC 33277 genome database) (Naito *et al.*, 2008)	M_r (kDa)	Accession number§
1	111	von Willebrand factor A domain protein (pgn0291)	134.65	34540039
2	90			
3	71	Pg-II fimbriae a (pgn0287)‖	60.79	22255314
4	51			
5	101			
6	53			
7	93			
8	77			
9	88	Lipoprotein, putative (pgn0289)	50.01	34540037
10	81	Immunoreactive 32 kDa antigen PG49 (pgn0290)	37.14	34540038

*Numbers refer to designations of protein bands in Fig. 3.

†Probabilities were based on the molecular weight search (MOWSE) scoring algorithm.

‡Protein-coding sequence.

§Nonredundant protein database at the NCBI (http://www.ncbi.nlm.nih.gov/).

‖Pg-II fimbriae a is the gene product of Pg-II fim a (designation from Ogawa *et al.*, 1995) from *P. gingivalis* strain BH18/10 and is another name for the Mfa1 protein, both of which were originally called minor fimbriae (Hamada *et al.*, 1996).

from the downstream three genes of *mfa2*. Because the association between the major and minor proteins seems to be stable during purification, the minor proteins identified seem to be inherent to Mfa1 fimbriae. Hereafter, the term 'accessory' rather than 'minor' proteins will be used. The gene product of *mfa2*, deduced to be a 37 kDa protein from the nucleotide sequence, was not detected in the purified Mfa1 fimbrial preparation (Fig. 3, lane Mfa1).

The localization of Mfa2 was examined using various cell fractions of the wild-type, its mutant (Δ*mfa2*) and the complemented strain (JI-3). As shown in Fig. 4(a), mature Mfa2 was detected as the 35 kDa protein in the whole-cell lysate and predominantly in the envelope fraction from the wild-type (Fig. 4a, lane 1 in WCL and Env), but not the mutant (Fig. 4a, lane 2 in WCL and Env). Much less Mfa2 was detected in the soluble fraction of 33277 (Fig. 4a, lane 1 in Sol). This is consistent with the observation that Mfa1 fimbriae, purified from the soluble fraction, did not carry Mfa2, as mentioned above. To demonstrate exact localization of Mfa2, the envelope fraction was then separated into the outer membrane and inner membrane fraction. As shown in Fig. 4(b), Mfa2 was detected mainly in the outer membrane fraction and was only slightly present in the inner membrane. The same was true of the *mfa2*-complemented strain JI-3, although much less Mfa2 appeared to be expressed. However, Mfa2 in JI-3 was strictly localized in the envelope and outer membrane fraction, strongly indicating that Mfa2 was originally present in the outer membrane. To confirm that the gene product of *mfa2* was absent in Mfa1 fimbriae, we carried out Western blotting with Mfa2 antiserum. As shown in Fig. 4(c), lane Mfa1 fimbriae, Mfa2 was not detected in Mfa1 fimbriae, although Mfa2 was clearly detected as a 35 kDa protein in whole-cell lysate (Fig. 4c, lane WCL). In addition, the localization of Mfa2 in the cell was

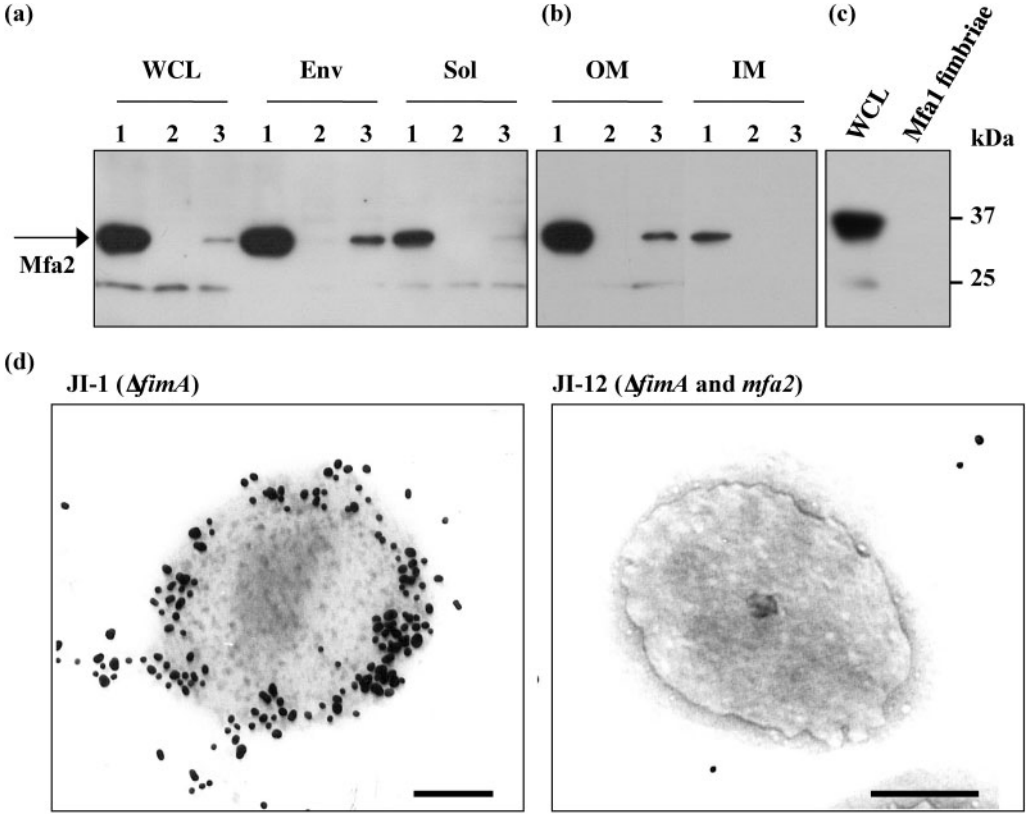

Fig. 4. Localization of Mfa2. (a) Localization of Mfa2 in the *P. gingivalis* cell. *P. gingivalis* whole-cell lysate (WCL), prepared by physical lysis, was fractionated into envelope (Env) and soluble (Sol) fractions, and Mfa2 was detected by Western blotting as described above. Lanes: 1, parental strain 33277; 2, JI-2; 3, JI-3. The band immunoreactive to anti-Mfa2 antiserum, which has a molecular mass of 24 kDa, appeared to cross-react with the antibody, but is unrelated to Mfa2 as it was present in the *mfa2* mutant. (b) Localization of Mfa2 in the outer membrane fraction. The envelope fractions were separated into outer membrane (OM) and inner membrane (IM) fractions, and Western blotting using Mfa2 antiserum was performed. The lanes are the same as for (a). (c) Absence of Mfa2 in the purified Mfa1 fimbriae. Mfa2 was detected by Western blotting. Lane WCL, whole-cell lysate of JI-1 (1 μg protein); lane Mfa1 fimbriae, the purified Mfa1 fimbriae from JI-1 (5 μg protein). (d) Immunogold electron microscopy. Ultra-thin sections of JI-1 (Δ*fimA*) and JI-12 (Δ*fimA* and Δ*mfa2*) cells were incubated with anti-Mfa2 serum, followed by labelling with 20 nm colloidal gold-labelled goat anti-rabbit serum. Bars, 200 nm.

demonstrated by immunogold electron microscopy (Fig. 4d, left panel). The cell surface of JI-1 was stained with gold particles. In contrast, JI-12 was only sparsely labelled (Fig. 4d, right panel). These data indicate that Mfa2 is localized on the cell surface, likely at the base of the Mfa1 fimbriae in the outer membrane.

Mfa1 and Mfa2 are associated with each other in cells

To determine whether Mfa2 interacts with Mfa1 in *P. gingivalis* cells, a whole-cell lysate, prepared by chemical lysis, was analysed by an immunoprecipitation assay. The whole-cell lysate from 33277 was immunoprecipitated by the addition of anti-Mfa1 or anti-Mfa2 serum, and the precipitate was separated by SDS-PAGE, followed by Western blotting with anti-Mfa2 or anti-Mfa1 serum. As shown in Fig. 5(a), proteins in immunoprecipitates with either antiserum were almost indistinguishable on SDS-PAGE gels, except for a 74 kDa protein band in lane 1, which appeared to be Mfa1, based on the results of subsequent Western blotting. Mfa2 was precipitated together with Mfa1 by the addition of anti-Mfa1 serum (Fig. 5c, lane 1). Also, Mfa1 was co-precipitated together with Mfa2 by the addition of anti-Mfa2 serum (Fig. 5b, lane 2). However, neither Mfa1 nor Mfa2 was precipitated by the addition of either pre-immune serum (data not shown) or anti-OmpA serum, which is specific to major outer membrane proteins (Pgm6/7) in this organism (lanes 3 in Fig. 5b, c), indicating that the co-precipitation of Mfa1 and Mfa2 with each antiserum is specific.

In order to confirm this association, immunogold microscopy, including double-labelling experiments, was performed using the two antisera. To do this, we raised specific antiserum to Mfa1 in chickens. Using this chicken anti-Mfa1 serum and 6 nm gold-labelled anti-chicken Ig, we first examined Mfa1 fimbriae of thin-sectioned JI-1 cells and then the association of Mfa1 fimbriae and Mfa2 using the two antisera, followed by incubation with 6 nm gold-labelled anti-chicken Ig and 20 nm gold-labelled anti-rabbit IgG, respectively. Many 6 nm gold particles (for Mfa1) were deposited around the cell (Fig. 5d) and appeared to be along filaments, and two types of gold particles were clearly detected around the cell in Fig. 5(e); apparently, several 20 nm gold particles (for Mfa2) were localized on the cell surface, as shown in Fig. 4(d), and were closely associated with an array of 6 nm gold particles representing Mfa1 fimbriae. These results are consistent with the idea that Mfa2 plays an anchoring role for the Mfa1 fimbriae in the outer membrane.

Electron micrographs of *P. gingivalis* cells and longer Mfa1 fimbriae purified from JI-12

Cells from 33277, JI-1 (Δ*fimA*) and JI-12 (Δ*fimA* and Δ*mfa2*) were negatively stained and examined by electron microscopy. Long filaments, characteristic of FimA fimbriae (Yoshimura *et al.*, 1984), were mainly seen on the surface of 33277 cells, as shown in Fig. 6(a). Only short filaments characteristic of Mfa1 fimbriae were detected in JI-1 (Fig. 6b), as shown elsewhere (Hamada *et al.*, 1996), and confirmed with Mfa1 antibodies (Park *et al.*, 2005). Interestingly, the double mutant JI-12 extruded long filaments from the cell surface (Fig. 6c). Furthermore, as mentioned above, mutant Mfa1 fimbriae tend to be easily released from the cell surface into the supernatant (Fig. 2a, b). Since our previous paper reported that the length of Mfa1 fimbriae purified from KDP98, another *fimA*-deficient mutant, is about 103 nm (Park *et al.*, 2005), they became remarkably longer in the mutant. The aberrant phenotype of Mfa1 fimbriae in JI-12 was restored to normal in an *mfa2*-complemented strain (JI-4) carrying pTCBex-*mfa2*, suggesting that the loss of *mfa2* was responsible for the aberrancy (Fig. 6d).

Longer Mfa1 fimbriae were easily purified from JI-12 cells by the mild washing method for FimA fimbriae, and long filaments similar to those partially purified from the culture supernatant (described above and data not shown) were again observed. Purified Mfa1 fimbriae from JI-12 indeed showed much longer filaments than those of parent Mfa1 fimbriae under electron microscopy (Fig. 7). The majority of fibres traversed throughout whole fields (Fig. 7a), reminiscent of long FimA fimbriae in 381 (Yoshimura *et al.*, 1984). On the other hand, the majority of fibres of the purified fimbriae from JI-1 (Δ*fimA*) were approximately 100 nm long (Fig. 7b), as seen in our previous observation (Park *et al.*, 2005). The length of Mfa1 fimbriae from JI-12 was estimated to be 1 μm or more (approximately 10 times longer than those of the parent), based on examination of five independent micrographs.

Autoaggregation activities of the *mfa2* mutants

Since Mfa1 fimbriae are reported to be involved in *P. gingivalis* autoaggregation (Lin *et al.*, 2006), autoaggregation activities in various strains were examined. As we previously reported (Nishiyama *et al.*, 2007), loss of FimA fimbriae was confirmed to result in much less autoaggregation (Fig. 8, compare open circles with filled circles), suggesting a reduced contribution of normal Mfa1 fimbriae to autoaggregation in this assay. Indeed, the mutant (JI-12) having longer Mfa1 fimbriae, but no FimA fimbriae, did not show a strong autoaggregation (Fig. 8, filled squares). However, the *mfa2* mutant, producing longer Mfa1 and having original long FimA fimbriae, resulted in a stronger autoaggregation than the wild-type (Fig. 8, compare open squares with open circles), implying a positive effect of long Mfa1 fimbriae. The *mfa2*-complemented strain JI-3 (equivalent to the wild-type) gave a similar autoaggregation pattern to the wild-type (compare open triangles with open circles). Another *mfa2*-complemented strain, JI-4 (equivalent to JI-1), was indistinguishable from JI-1 in the autoaggregation pattern (compare filled triangles with filled circles), suggesting that no matter how long they are, Mfa1 fimbriae alone contribute marginally to autoaggregation.

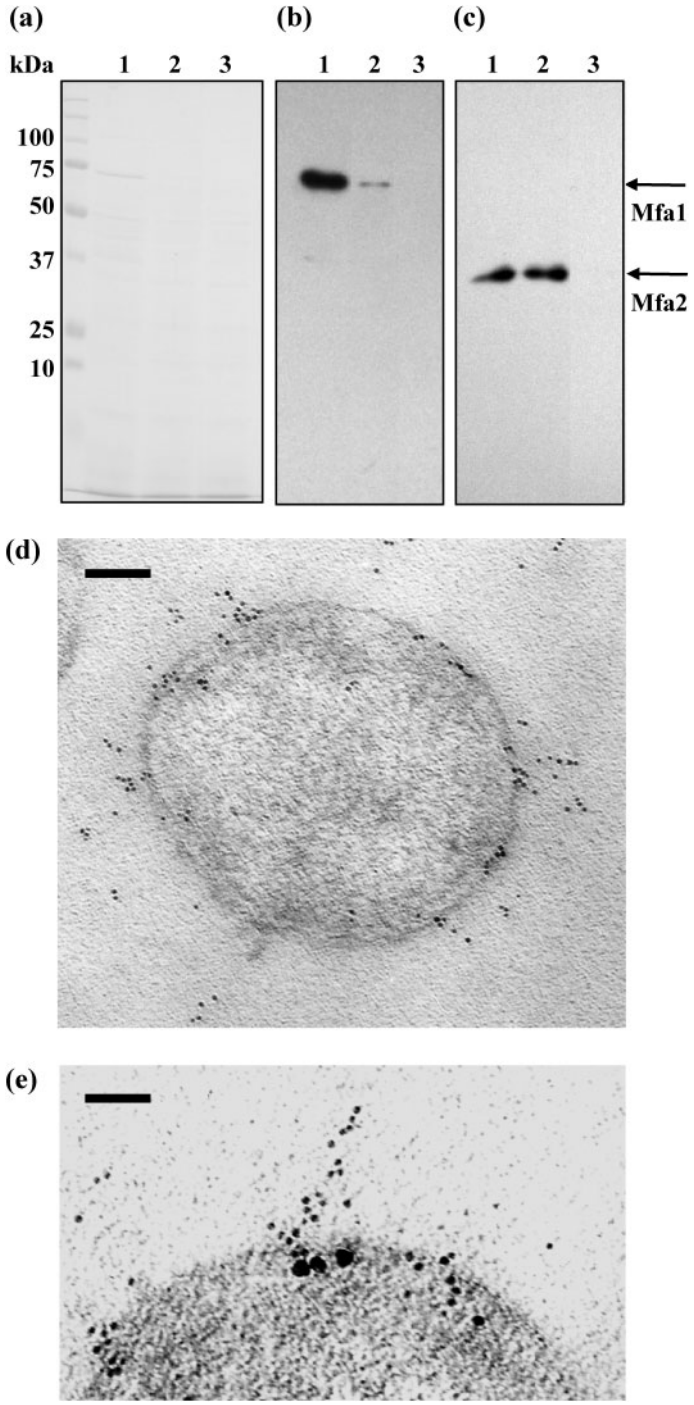

Fig. 5. Physical association and co-localization between Mfa1 and Mfa2. Mfa1 or Mfa2 was immunoprecipitated from whole-cell lysate of 33277 with anti-Mfa1 or anti-Mfa2 serum. The precipitates were separated by SDS-PAGE (a), followed by Western blotting using either anti-Mfa1 (b) or anti-Mfa2 serum (c). Lanes: 1, 33277 precipitate with anti-Mfa1; 2, 33277 precipitate with anti-Mfa2; 3, 33277 precipitate with anti-OmpA (Pgm6/7) as a negative control. The positions of Mfa1, Mfa2 and molecular mass markers are indicated. (d) Single-labelled, immunogold electron microscopy. Ultra-thin sections of JI-1 (Δ*fimA*) were reacted with chicken anti-Mfa1, followed by 6 nm gold-labelled anti-chicken Ig. Bar, 100 nm. (e) Double-labelling immunogold microscopy. The sections were first reacted with chicken anti-Mfa1 and rabbit anti-Mfa2 serum, followed by incubation with 6 nm gold-labelled anti-chicken Ig and 20 nm gold-labelled anti-rabbit IgG. Bar, 50 nm.

Transcriptional analysis of the *mfa1* and downstream genes

Mfa1 and related minor proteins are encoded in a chromosomal region containing five genes that have the same transcriptional direction (Fig. 1 and Fig. 9a). We extended our earlier analysis of *mfa1* and *mfa2* co-transcription (Chung *et al.*, 2000) by RT-PCR throughout the *mfa1*–pgn0291 cluster in 33277 using the primers listed in Table 2. Amplification with intragenic primer pairs for the genes *mfa1*–pgn0291 demonstrated that each of the genes was expressed (Fig. 9b, lanes 1–5 under cDNA). The same primers were used in pairs that spanned each intergenic region. Results in Fig. 9(b), lanes 6–10 under cDNA, show that mRNAs were detected that spanned *mfa1* and *mfa2*, *mfa1* and pgn0289, *mfa2* and pgn0289, *mfa2* and pgn0290, and pgn0289 and pgn0290. The mRNA that spanned *mfa1* and pgn0289 was detected, although the detected band was weak (Fig. 9b, lane 7 under cDNA). This is presumably due to its being the longest target, which

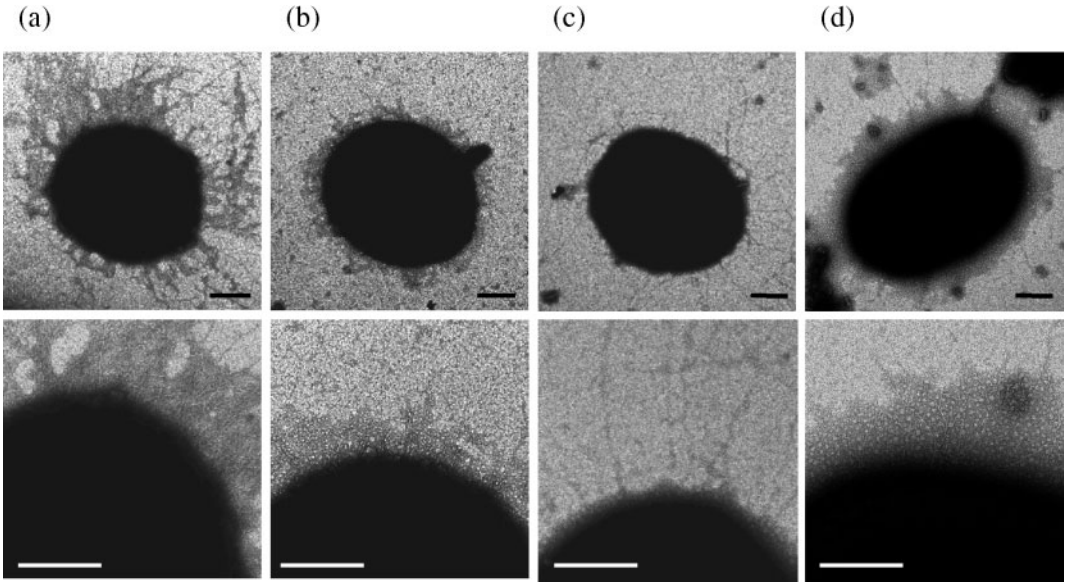

Fig. 6. Electron micrographs of the cell and cell surface of the parental and mutant strains. A part of the cell surface of each strain is enlarged in the lower panel. (a) ATCC 33277, (b) JI-1 (Δ*fimA*), (c) JI-12 (Δ*fimA* and Δ*mfa2*), (d) complemented strain JI-4. All strains were negatively stained with 1 % (w/v) ammonium molybdate. Bars, 100 nm.

may be close to the PCR detection limit. However, *P. gingivalis* mRNA that spans pgn0290 and pgn0291 was not detected, although mRNA of pgn0291 itself was detected (Fig. 9b, lane 11 under cDNA). These data indicate that the *mfa1* operon can be transcribed as a four-gene polycistronic message encompassing *mfa1*–pgn0290.

DISCUSSION

P. gingivalis ATCC 33277 possesses two types of morphologically distinct long (FimA) and short (Mfa1) fimbriae (Naito *et al.*, 2008), although both are thin, single-stranded filaments with a diameter of 5–6.5 nm (Park *et al.*, 2005;

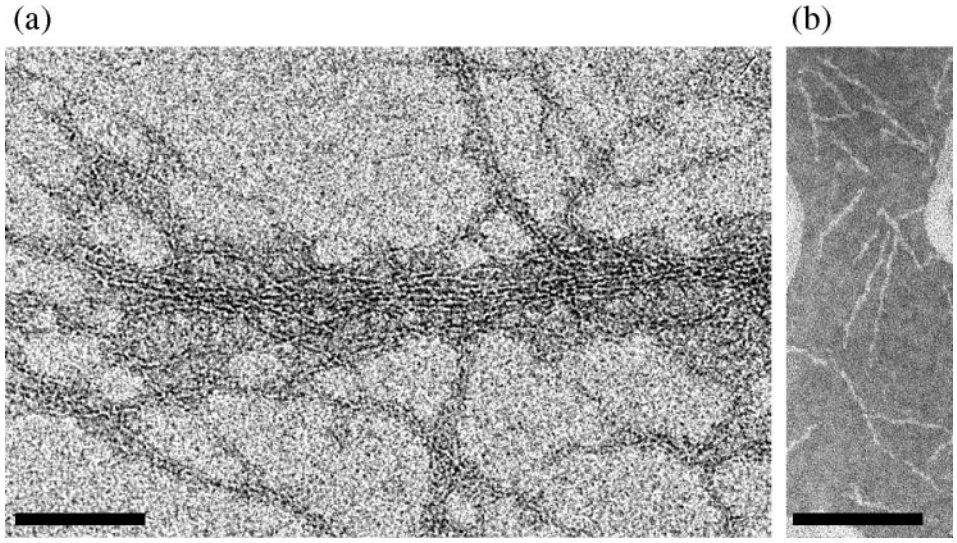

Fig. 7. Effect of *mfa2* on the Mfa1 fimbriae length. (a) Electron micrograph of the purified Mfa1 fimbriae from JI-12 (Δ*fimA* and Δ*mfa2*) negatively stained with 1 % (w/v) ammonium molybdate. The samples were observed under a Carl-Zeiss LEO LIBRA120 electron microscope. Bar, 100 nm. (b) Electron micrograph of the purified Mfa1 fimbriae from JI-1 (Δ*fimA*). The sample was negatively stained with 1 % (w/v) ammonium molybdate and observed under a JEM-1200EX (JEOL). Bar, 100 nm.

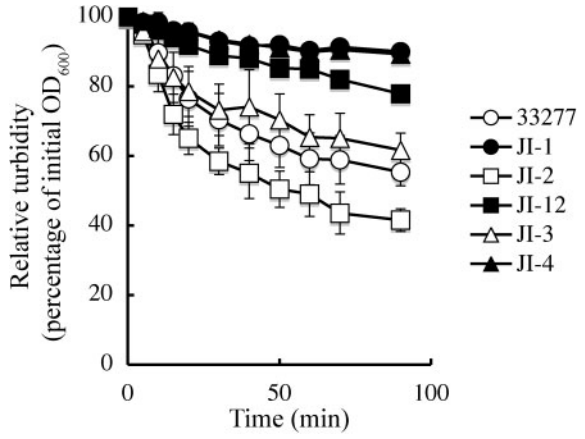

Fig. 8. Time-course of autoaggregation of the wild-type and various mutants. The OD_{600} value of each cell suspension was measured at the indicated time points. Relative turbidities, defined as the relative OD_{600} value (as a percentage) normalized to the initial value of each suspension, are plotted against incubation time. All assays were performed in triplicate and the means ± SD are shown. ○, Wild-type strain ATCC 33277; ●, JI-1 (Δ*fimA*); □, JI-2 (Δ*mfa2*); ■, JI-12 (Δ*fimA* and Δ*mfa2*); △, JI-3 (JI-2 containing pTCBex-*mfa2*, complemented strain); ▲, JI-4 (JI-12 containing pTCBex-*mfa2*, complemented strain).

Yoshimura *et al.*, 1984). In order to investigate the role of *mfa2*, downstream of *mfa1*, experiments were conducted in a *fimA*-knockout background to prevent any misidentification of fimbriae of aberrant length. Indeed, double mutant JI-12 (Δ*fimA* and Δ*mfa2*) clearly formed unusual longer filaments, easily shed from the cell surface, and strains JI-3 and JI-4 complemented with the wild-type *mfa2* allele recovered the phenotype of the parent. Collectively, these results indicate that *mfa2* plays a role in the normal formation of Mfa1 filaments of short, uniform size (Park *et al.*, 2005) that are tightly bound to the cell surface. Longer Mfa1 fimbriae emerged on the cell surface of JI-2 (Δ*mfa2*) and induced enhanced autoaggregation activity, to some extent presumably in collaboration with long FimA fimbriae, although Mfa1 fimbriae themselves did not contribute much to autoaggregation in the absence of FimA fimbriae [Fig. 8, see JI-1 (Δ*fimA*) and JI-12 (Δ*fimA* and Δ*mfa2*)].

Antibodies to rMfa2 showed that mature Mfa2 resided in the outer membrane, consistent with the concept that Mfa2 plays a role as an anchor in order to tightly connect filaments to the outer membrane following polymerization of fimbrilins into filaments. Thus, Mfa2 may play roles as an anchor and as a regulator of their length. We also showed that purified Mfa1 fimbriae have at least three accessory proteins, as do FimA fimbriae (Nishiyama *et al.*, 2007; Yoshimura *et al.*, 1993), and that Mfa2 is not present as an accessory component (Figs 3 and 4c, Table 3). However, Mfa2 was found to associate with Mfa1 fimbrilin in cells and was likely present on the base of the Mfa1 fimbrial structure (Fig. 5), supporting an anchor function for Mfa2. Whole-cell lysates for immunoprecipitation were prepared by a chemical lysis method using a commercial solution including a detergent mix, different from that for purification of Mfa1 fimbriae. For purification of Mfa1 fimbriae, bacterial cells were physically disrupted with a French pressure cell (Park *et al.*, 2005). We assume that harsh, mechanical disruption of bacterial cells, such as by French press, tends to leave Mfa2 in the outer membrane and to release filaments of Mfa1 fimbriae into solution, which may reflect the structure and function of Mfa2 in the membrane.

By RT-PCR, *mfa1* and *mfa2* (equivalent to pgn0288) were confirmed to be co-transcribed, and the genes pgn0289, pgn0290 and pgn0291, encoding the three accessory components detected in this study, were shown to be indeed transcribed in cells. In addition, *mfa1*–pgn0290 appeared to be co-transcribed. We also examined expression of three downstream genes from *mfa2* in JI-2 (Δ*mfa2*), because of the possibility that the mutation in *mfa2* could result in a polar effect on these genes. RT-PCR products of the expected sizes for pgn0289, pg0290 and pgn0291 were detected from JI-2. Moreover, longer Mfa1 fimbriae purified from JI-12 (Δ*fimA* and Δ*mfa2*) also contained three accessory proteins as their gene products (data not shown). Taken together, the three genes pgn0289, pg0290 and pgn0291, which were transcribed as a large mRNA spanning *mfa1* to pgn0290 (Fig. 9), seem to be at least in part independent of upstream *mfa2* and partially expressed, although further work is needed to confirm this.

A similarity between FimA and Mfa1 fimbriae in *P. gingivalis* is notable with regard to the possession of three minor protein components, and the presence of similar gene orders and clusters consisting of five genes. However, FimA and Mfa1 have different biological activities and may thus be operational in differing environmental situations. The gene corresponding to *mfa2* in the *fimA* cluster has been shown to be ORF1 (equivalent to pgn0181 in 33277 or pg2133 in W83), located between *fimA* and *fimC* in 33277 and 381 (Naito *et al.*, 2008; Nishikawa *et al.*, 2004; Nishiyama *et al.*, 2007), and its gene product and function have yet to be identified. However, the *mfa2*-corresponding gene (designated *fimB*) appears to be truncated by a point mutation, creating a stop codon at the middle portion in both strains (Naito *et al.*, 2008; Nishiyama *et al.*, 2007; Watanabe *et al.*, 1996), but not in W83 (Nelson *et al.*, 2003) or OMZ 314 (type II in *fimA*) (Kato *et al.*, 2007). Therefore, ORF1 in 33277 and 381 encodes a putative 15 kDa protein (Nishiyama *et al.*, 2007), but the corresponding genes (pg2133 for W83) in W83 and OMZ 314 encode a putative 34 kDa protein (Kato *et al.*, 2007; Nelson *et al.*, 2003), a size equivalent to Mfa2.

We assume that both strain 33277 and strain 381 carry FimA fimbriae (both *fimA* genotype I), easily shed from the cell surface, with unusually long filaments due to the mutation in the *fimB* gene, equivalent to *mfa2* in Mfa1 fimbriae. Evidence for this is as follows. (1) The two strains are believed to be siblings. (2) We have not thus far

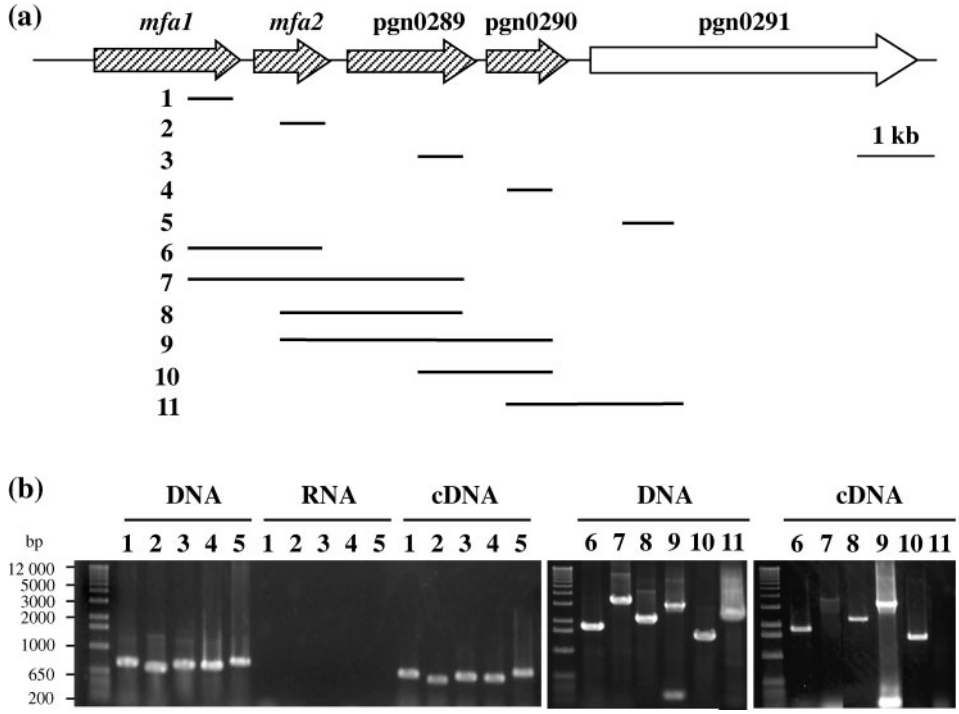

Fig. 9. Transcriptional analysis of the genes for Mfa1 fimbrial components. (a) The predicted PCR fragments from *mfa1* to pgn0291 are indicated as thin lines at the right side of the numbers (1–11). The possible operon is shaded. Gene annotation corresponds to the 33277 genome database. (b) RT-PCR of 33277 mRNAs from *mfa1* to pgn0291. RT-PCR amplification of intragenic and intergenic segments within the *mfa1* gene cluster was carried out with primer pairs listed in Table 2. Results labelled as DNA indicate that PCR was carried out using chromosomal DNA as a template, showing that each primer set was appropriate, and those labelled as RNA indicate that RT-PCR was carried out without reverse transcriptase as negative controls, showing that the RNA preparation was pure, without contamination of DNA. Therefore, results labelled as cDNA indicate the presence or absence of mRNA. The lane numbers correspond to those in panel (a). Lanes: 1, primers for *mfa1*; 2, primers for *mfa2*; 3, primers for pgn0289; 4, primers for pgn0290; 5, primers for pgn0291; 6, primers for a region spanning *mfa1* and *mfa2*; 7, primers for a region spanning *mfa1* and pgn0289; 8, primers for a region spanning *mfa2* and pgn0289; 9, primers for a region spanning *mfa2* and pgn0290; 10, primers for a region spanning pgn0289 and pgn0290; 11, primers for a region spanning pgn0290 and pgn0291.

encountered any *P. gingivalis* strains carrying FimA fimbriae that could be shed from the cell surface by the mild, selective washing method, except for the two strains 33277 and 381 (Yoshimura *et al.*, 1984). (3) FimA fimbriae in several strains, OMZ314, HW24D1 (both genotype II), MPWIb-01 (type Ib, a close variant of genotype I in *fimA*, kindly provided by M. Miura, Kyushu University) and ESO101 (genotype I) (Kato *et al.*, 2007; Miura *et al.*, 2005; Nakagawa *et al.*, 2002), were not selectively solubilized from the cell surface by the washing method, which is a reliable procedure for isolation from 33277 and 381 (our unpublished data). (4) In all these strains, most of the FimA and Mfa1 fimbriae can be released into the soluble fraction by French pressure disruption (Murakami *et al.*, 2002). (5) It is also pertinent to mention that complete deletion of ORF1 (pgn0181) does not produce any apparent differences in FimA fimbriae in 33277 (Nishiyama *et al.*, 2007). Taken together, these data suggest that *mfa2* and *fimB* play a similar role in the Mfa1 and FimA fimbriae of *P. gingivalis*, and that strains 33277 and 381 may be natural mutants in FimA fimbriae. However, this hypothesis needs to be examined further.

Fimbriae, pili or curli are adhesive hair-like organelles that project from the cell surface of a wide variety of Gram-negative as well as Gram-positive bacteria (Barnhart & Chapman, 2006; Capitani *et al.*, 2006; Pizarro-Cerda & Cossart, 2006). The morphogenesis or biogenesis of some of these, especially in *E. coli*, has been extensively studied (Kuehn *et al.*, 1994; Piatek *et al.*, 2005; Wu & Fives-Taylor, 2001), and several systems such as the chaperone/usher pathway (Piatek *et al.*, 2005), type II secretion (Hansen & Forest, 2006) and secretion/nucleation (Barnhart & Chapman, 2006) have been proposed for their generation. PapH, similar to Mfa2, with roles in anchoring fimbriae to cells and in modulating their length, has been reported in *E. coli* Pap pili (Baga *et al.*, 1987; Verger *et al.*, 2006). *papH* is located adjacent to and downstream of *papA*, which encodes the major pilin subunit, a similar situation to the

configuration of *mfa1* and *mfa2*. The corresponding gene *fimI*, downstream of *fimA* in *E. coli* type I pili, has not yet been assigned a function (Sauer *et al.*, 2004; Schilling *et al.*, 2001). Mfa1 and FimA fimbriae in *P. gingivalis* are structurally, genetically and biosynthetically different from those in *E. coli* (Nishiyama *et al.*, 2007; Yoshimura *et al.*, 1984, 1993). Therefore, elucidation of the structure and function of Mfa2 and ORF1 could bring new insights in fimbrial research that extend beyond the paradigm of *E. coli*.

P. gingivalis, a periodontopathogen, proteomically most similar to *B. thetaiotaomicron* and *B. fragilis*, also a member of the *Cytophaga–Flavobacteria–Bacteroides* group (Nelson *et al.*, 2003), appears to use a novel fimbrial biogenesis system via a lipoprotein precursor and using Arg-gingipain (RGP), a major arginine-specific proteinase, as the maturation enzyme (Shoji *et al.*, 2004). Our findings on Mfa2 function do not necessarily conflict with the lipoprotein precursor biogenesis as proposed previously (Shoji *et al.*, 2004). Lipoprotein precursors of fimbrilin could be processed by RGP in the outer membrane, followed by assembly into filaments with the involvement of Mfa2.

In conclusion, our study has highlighted that Mfa2, the product of *mfa2* downstream of the major subunit gene *mfa1*, may be involved as an anchor of filaments as well as a regulator in the filament length of Mfa1 fimbriae in *P. gingivalis*.

ACKNOWLEDGEMENTS

We thank Kunihiko Kobayashi (College of Life and Health Sciences, Chubu University) and Yuka Mitamura-Kondo (Electron Microscopy Laboratory, Aichi-Gakuin University) for their helpful, technical advice. We also thank the Institute for Genomic Research (TIGR) for making the *P. gingivalis* W83 genomic sequence freely available to the public. This work was supported by Grants-in-Aid for Scientific Research (20890248 to Y. H., 15591958 and 20592165 to Y. M., 19592139 to K. N. and 15591957 to F. Y.) from the Japan Society for the Promotion of Science (JSPS) and the AGU High-Tech Research Center Project and Strategic Research AGU-Platform Formation from The Ministry of Education, Culture, Sports, Science and Technology, Japan, the Furukawa foundation to Y. H., and DE12505 from the National Institute of Dental and Craniofacial Research (NIDCR) (to R. J. L.).

REFERENCES

Andrian, E., Grenier, D. & Rouabhia, M. (2006). *Porphyromonas gingivalis*-epithelial cell interactions in periodontitis. *J Dent Res* **85**, 392–403.

Arai, M., Hamada, N. & Umemoto, T. (2000). Purification and characterization of a novel secondary fimbrial protein from *Porphyromonas gingivalis* strain 381. *FEMS Microbiol Lett* **193**, 75–81.

Baga, M., Norgren, M. & Normark, S. (1987). Biogenesis of *E. coli* Pap pili: *papH*, a minor pilin subunit involved in cell anchoring and length modulation. *Cell* **49**, 241–251.

Barnhart, M. M. & Chapman, M. R. (2006). Curli biogenesis and function. *Annu Rev Microbiol* **60**, 131–147.

Capitani, G., Eidam, O., Glockshuber, R. & Grutter, M. G. (2006). Structural and functional insights into the assembly of type 1 pili from *Escherichia coli*. *Microbes Infect* **8**, 2284–2290.

Chung, W. O., Demuth, D. R. & Lamont, R. J. (2000). Identification of a *Porphyromonas gingivalis* receptor for the *Streptococcus gordonii* SspB protein. *Infect Immun* **68**, 6758–6762.

Dasanayake, A. P., Russell, S., Boyd, D., Madianos, P. N., Forster, T. & Hill, E. (2003). Preterm low birth weight and periodontal disease among African Americans. *Dent Clin North Am* **47**, 115–125.

Fletcher, H. M., Morgan, R. M. & Macrina, F. L. (1997). Nucleotide sequence of the *Porphyromonas gingivalis* W83 *recA* homolog and construction of a *recA*-deficient mutant. *Infect Immun* **65**, 4592–4597.

Gardner, R. G., Russell, J. B., Wilson, D. B., Wang, G. R. & Shoemaker, N. B. (1996). Use of a modified *Bacteroides–Prevotella* shuttle vector to transfer a reconstructed β-1,4-D-endoglucanase gene into *Bacteroides uniformis* and *Prevotella ruminicola* B_14. *Appl Environ Microbiol* **62**, 196–202.

Gibson, F. C., III, Yumoto, H., Takahashi, Y., Chou, H. H. & Genco, C. A. (2006). Innate immune signaling and *Porphyromonas gingivalis*-accelerated atherosclerosis. *J Dent Res* **85**, 106–121.

Hajishengallis, G., Martin, M., Sojar, H. T., Sharma, A., Schifferle, R. E., DeNardin, E., Russell, M. W. & Genco, R. J. (2002). Dependence of bacterial protein adhesins on Toll-like receptors for proinflammatory cytokine induction. *Clin Diagn Lab Immunol* **9**, 403–411.

Hall, L. M., Fawell, S. C., Shi, X., Faray-Kele, M. C., Aduse-Opoku, J., Whiley, R. A. & Curtis, M. A. (2005). Sequence diversity and antigenic variation at the *rag* locus of *Porphyromonas gingivalis*. *Infect Immun* **73**, 4253–4262.

Hamada, N., Sojar, H. T., Cho, M. I. & Genco, R. J. (1996). Isolation and characterization of a minor fimbria from *Porphyromonas gingivalis*. *Infect Immun* **64**, 4788–4794.

Hamada, N., Watanabe, K., Arai, M., Hiramine, H. & Umemoto, T. (2002). Cytokine production induced by a 67-kDa fimbrial protein from *Porphyromonas gingivalis*. *Oral Microbiol Immunol* **17**, 197–200.

Hansen, J. K. & Forest, K. T. (2006). Type IV pilin structures: insights on shared architecture, fiber assembly, receptor binding and type II secretion. *J Mol Microbiol Biotechnol* **11**, 192–207.

Hasegawa, Y., Nishiyama, S., Nishikawa, K., Kadowaki, T., Yamamoto, K., Noguchi, T. & Yoshimura, F. (2003). A novel type of two-component regulatory system affecting gingipains in *Porphyromonas gingivalis*. *Microbiol Immunol* **47**, 849–858.

Hayashi, J., Nishikawa, K., Hirano, R., Noguchi, T. & Yoshimura, F. (2000). Identification of a two-component signal transduction system involved in fimbriation of *Porphyromonas gingivalis*. *Microbiol Immunol* **44**, 279–282.

Hiramine, H., Watanabe, K., Hamada, N. & Umemoto, T. (2003). *Porphyromonas gingivalis* 67-kDa fimbriae induced cytokine production and osteoclast differentiation utilizing TLR2. *FEMS Microbiol Lett* **229**, 49–55.

Hongo, H., Osano, E., Ozeki, M., Onoe, T., Watanabe, K., Honda, O., Tani, H., Nakamura, H. & Yoshimura, F. (1999). Characterization of an outer membrane protein gene, *pgmA*, and its gene product from *Porphyromonas gingivalis*. *Microbiol Immunol* **43**, 937–946.

Hongyo, H., Kurihara, H., Kokeguchi, S., Miyamoto, M., Maeda, H., Hayakawa, M., Abiko, Y., Takashiba, S. & Murayama, Y. (1997). Molecular cloning and characterization of the gene encoding 53 kD outer membrane protein of *Porphyromonas gingivalis*. *Microbios* **92**, 47–57.

Hongyo, H., Kokeguchi, S., Kurihara, H., Miyamoto, M., Maeda, H., Takashiba, S. & Murayama, Y. (1998). Comparative study of two outer membrane protein genes from *Porphyromonas gingivalis*. *Microbios* **95**, 91–100.

Jenkinson, H. F. & Lamont, R. J. (2005). Oral microbial communities in sickness and in health. *Trends Microbiol* **13**, 589–595.

Kato, T., Kawai, S., Nakano, K., Inaba, H., Kuboniwa, M., Nakagawa, I., Tsuda, K., Omori, H., Ooshima, T. & other authors (2007). Virulence of *Porphyromonas gingivalis* is altered by substitution of fimbria gene with different genotype. *Cell Microbiol* **9**, 753–765.

Kolenbrander, P. E., Andersen, R. N., Blehert, D. S., Egland, P. G., Foster, J. S. & Palmer, R. J., Jr (2002). Communication among oral bacteria. *Microbiol Mol Biol Rev* **66**, 486–505.

Kuehn, M. J., Jacob-Dubuisson, F., Dodson, K., Slonim, L., Striker, R. & Hultgren, S. J. (1994). Genetic, biochemical, and structural studies of biogenesis of adhesive pili in bacteria. *Methods Enzymol* **236**, 282–306.

Lamont, R. J. & Jenkinson, H. F. (1998). Life below the gum line: pathogenic mechanisms of *Porphyromonas gingivalis*. *Microbiol Mol Biol Rev* **62**, 1244–1263.

Lamont, R. J., El-Sabaeny, A., Park, Y., Cook, G. S., Costerton, J. W. & Demuth, D. R. (2002). Role of the *Streptococcus gordonii* SspB protein in the development of *Porphyromonas gingivalis* biofilms on streptococcal substrates. *Microbiology* **148**, 1627–1636.

Lin, X., Wu, J. & Xie, H. (2006). *Porphyromonas gingivalis* minor fimbriae are required for cell–cell interactions. *Infect Immun* **74**, 6011–6015.

Masuda, T., Murakami, Y., Noguchi, T. & Yoshimura, F. (2006). Effects of various growth conditions in a chemostat on expression of virulence factors in *Porphyromonas gingivalis*. *Appl Environ Microbiol* **72**, 3458–3467.

Miura, M., Hamachi, T., Fujise, O. & Maeda, K. (2005). The prevalence and pathogenic differences of *Porphyromonas gingivalis fimA* genotypes in patients with aggressive periodontitis. *J Periodontal Res* **40**, 147–152.

Murakami, Y., Imai, M., Nakamura, H. & Yoshimura, F. (2002). Separation of the outer membrane and identification of major outer membrane proteins from *Porphyromonas gingivalis*. *Eur J Oral Sci* **110**, 157–162.

Nagano, K., Read, E. K., Murakami, Y., Masuda, T., Noguchi, T. & Yoshimura, F. (2005). Trimeric structure of major outer membrane proteins homologous to OmpA in *Porphyromonas gingivalis*. *J Bacteriol* **187**, 902–911.

Nagano, K., Murakami, Y., Nishikawa, K., Sakakibara, J., Shimozato, K. & Yoshimura, F. (2007). Characterization of RagA and RagB in *Porphyromonas gingivalis*: study using gene-deletion mutants. *J Med Microbiol* **56**, 1536–1548.

Naito, M., Hirakawa, H., Yamashita, A., Ohara, N., Shoji, M., Yukitake, H., Nakayama, K., Toh, H., Yoshimura, F. & other authors (2008). Determination of the genome sequence of *Porphyromonas gingivalis* strain ATCC 33277 and genomic comparison with strain W83 revealed extensive genome rearrangements in *P. gingivalis*. *DNA Res* **15**, 215–225.

Nakagawa, I., Amano, A., Ohara-Nemoto, Y., Endoh, N., Morisaki, I., Kimura, S., Kawabata, S. & Hamada, S. (2002). Identification of a new variant of *fimA* gene of *Porphyromonas gingivalis* and its distribution in adults and disabled populations with periodontitis. *J Periodontal Res* **37**, 425–432.

Nelson, K. E., Fleischmann, R. D., DeBoy, R. T., Paulsen, I. T., Fouts, D. E., Eisen, J. A., Daugherty, S. C., Dodson, R. J., Durkin, A. S. & other authors (2003). Complete genome sequence of the oral pathogenic bacterium *Porphyromonas gingivalis* strain W83. *J Bacteriol* **185**, 5591–5601.

Nishikawa, K., Yoshimura, F. & Duncan, M. J. (2004). A regulation cascade controls expression of *Porphyromonas gingivalis* fimbriae via the FimR response regulator. *Mol Microbiol* **54**, 546–560.

Nishiyama, S., Murakami, Y., Nagata, H., Shizukuishi, S., Kawagishi, I. & Yoshimura, F. (2007). Involvement of minor components associated with the FimA fimbriae of *Porphyromonas gingivalis* in adhesive functions. *Microbiology* **153**, 1916–1925.

Ogawa, T., Mori, H., Yasuda, K. & Hasegawa, M. (1994). Molecular cloning and characterization of the genes encoding the immunoreactive major cell-surface proteins of *Porphyromonas gingivalis*. *FEMS Microbiol Lett* **120**, 23–30.

Ogawa, T., Yasuda, K., Yamada, K., Mori, H., Ochiai, K. & Hasegawa, M. (1995). Immunochemical characterisation and epitope mapping of a novel fimbrial protein (Pg-II fimbria) of *Porphyromonas gingivalis*. *FEMS Immunol Med Microbiol* **11**, 247–255.

Park, Y., Simionato, M. R., Sekiya, K., Murakami, Y., James, D., Chen, W., Hackett, M., Yoshimura, F., Demuth, D. R. & Lamont, R. J. (2005). Short fimbriae of *Porphyromonas gingivalis* and their role in coadhesion with *Streptococcus gordonii*. *Infect Immun* **73**, 3983–3989.

Piatek, R., Zalewska, B., Bury, K. & Kur, J. (2005). The chaperone–usher pathway of bacterial adhesin biogenesis – from molecular mechanism to strategies of anti-bacterial prevention and modern vaccine design. *Acta Biochim Pol* **52**, 639–646.

Pizarro-Cerda, J. & Cossart, P. (2006). Bacterial adhesion and entry into host cells. *Cell* **124**, 715–727.

Sakakibara, J., Nagano, K., Murakami, Y., Higuchi, N., Nakamura, H., Shimozato, K. & Yoshimura, F. (2007). Loss of adherence ability to human gingival epithelial cells in S-layer protein-deficient mutants of *Tannerella forsythensis*. *Microbiology* **153**, 866–876.

Sauer, F. G., Remaut, H., Hultgren, S. J. & Waksman, G. (2004). Fiber assembly by the chaperone–usher pathway. *Biochim Biophys Acta* **1694**, 259–267.

Schilling, J. D., Mulvey, M. A. & Hultgren, S. J. (2001). Structure and function of *Escherichia coli* type 1 pili: new insight into the pathogenesis of urinary tract infections. *J Infect Dis* **183** (Suppl. 1), S36–S40.

Shoji, M., Naito, M., Yukitake, H., Sato, K., Sakai, E., Ohara, N. & Nakayama, K. (2004). The major structural components of two cell surface filaments of *Porphyromonas gingivalis* are matured through lipoprotein precursors. *Mol Microbiol* **52**, 1513–1525.

Socransky, S. S. & Haffajee, A. D. (2005). Periodontal microbial ecology. *Periodontol 2000* **38**, 135–187.

Suzuki, Y., Yoshimura, F., Takahashi, K., Tani, H. & Suzuki, T. (1988). Detection of fimbriae and fimbrial antigens on the oral anaerobe *Bacteroides gingivalis* by negative staining and serological methods. *J Gen Microbiol* **134**, 2713–2720.

Takahashi, Y., Davey, M., Yumoto, H., Gibson, F. C., III & Genco, C. A. (2006). Fimbria-dependent activation of pro-inflammatory molecules in *Porphyromonas gingivalis* infected human aortic endothelial cells. *Cell Microbiol* **8**, 738–757.

Verger, D., Miller, E., Remaut, H., Waksman, G. & Hultgren, S. (2006). Molecular mechanism of P pilus termination in uropathogenic *Escherichia coli*. *EMBO Rep* **7**, 1228–1232.

Watanabe, K., Onoe, T., Ozeki, M., Shimizu, Y., Sakayori, T., Nakamura, H. & Yoshimura, F. (1996). Sequence and product analyses of the four genes downstream from the fimbrilin gene (*fimA*) of the oral anaerobe *Porphyromonas gingivalis*. *Microbiol Immunol* **40**, 725–734.

Wu, H. & Fives-Taylor, P. M. (2001). Molecular strategies for fimbrial expression and assembly. *Crit Rev Oral Biol Med* **12**, 101–115.

Yoshimura, F., Takahashi, K., Nodasaka, Y. & Suzuki, T. (1984). Purification and characterization of a novel type of fimbriae from the oral anaerobe *Bacteroides gingivalis*. *J Bacteriol* **160**, 949–957.

Yoshimura, F., Watanabe, K., Takasawa, T., Kawanami, M. & Kato, H. (1989). Purification and properties of a 75-kilodalton major protein, an immunodominant surface antigen, from the oral anaerobe *Bacteroides gingivalis*. *Infect Immun* **57**, 3646–3652.

Yoshimura, F., Takahashi, Y., Hibi, E., Takasawa, T., Kato, H. & Dickinson, D. P. (1993). Proteins with molecular masses of 50 and 80 kilodaltons encoded by genes downstream from the fimbrilin gene (*fimA*) are components associated with fimbriae in the oral anaerobe *Porphyromonas gingivalis*. *Infect Immun* **61**, 5181–5189.

Yoshimura, F., Murakami, Y., Nishikawa, K., Hasegawa, Y. & Kawaminami, S. (2009). Surface components of *Porphyromonas gingivalis*. *J Periodontal Res* **44**, 1–12.

Edited by: M. A. Curtis